



## A novel Two-Port MIMO Antenna with Enhanced Isolation and Diversity Parameters for Wireless Applications

Satish Kumar Kannale<sup>1\*</sup> and N M Biradar<sup>2</sup>

<sup>1</sup>Research Scholar, Department of Electronics and communication Engineering, VTU Belagavi (Karnataka), INDIA.

<sup>2</sup>Principal, BKIT, Bhalki (Karnataka), INDIA.

(Corresponding author: Satish Kumar Kannale\*)

(Received 02 March 2023, Revised 21 April 2023, Accepted 31 April 2023)

(Published by Research Trend, Website: [www.researchtrend.net](http://www.researchtrend.net))

**ABSTRACT:** Wireless-enabled gadgets pack a lot of functionality into a small package, which necessitates much bandwidth for speedier data transfer. This paper discusses the characteristics of two-element multiple-input and multiple output (MIMO) antenna systems operating in ultra-wideband (UWB). The close proximity of the antenna components results in high mutual coupling. The unique chain-structured parasitic element is introduced on the radiator to enhance isolation and acts as a decoupling structure. The physical dimension of the substrate is 21.5×34×1.6 mm<sup>3</sup>. The addition of a decoupling structure enhances isolation by more than 15 dB for the working frequency range of 4.5-13 GHz. Additionally, the diversity characteristics of MIMO are examined, (Envelope Correlation Coefficient (ECC)<0.05 dB, Mean Effective Gain (MEG)<3dB, Total Active reflection coefficient (TARC) <-10 dB ratio, and CCL< 0.4 bps/Hz outcome confirming that the suggested MIMO architecture is well-suited for applications involving wireless communication.

**Keywords:** MIMO, isolation, chain-structured parasitic element, ECC, DG, CCL

**Abbreviations:** MIMO. Multiple-input and multiple outputs; PCM, UWB ultra wide bandmen, Mean Effective Gain.

### I. INTRODUCTION

Wireless communication is the most preferred channel for transmitting and receiving information in modern portable electronic devices. These devices offer multiple features that demand large bandwidth for seamless operation. The ultra-wideband (UWB) technology provides 7.5 GHz unlicensed bandwidth in the frequency range of 3.1 to 10.6 GHz [1]. In recent years UWB has been widely studied and used in near-field communication due to its outstanding features like low power and large frequency spectrum. The short pulses used in UWB communication cause multipath fading due to diffraction [2]. Multiple-input and multiple output (MIMO) technology are used in conjunction with UWB to take advantage of UWB and overcome the issue of multipath channel fading. MIMO technology is a major key factor in the exponential growth of wireless communication technology. The MIMO provides extensive coverage, improved spectral efficiency, enhanced QoS, and high-speed communication. The multiple antennas at the transceivers help improve the spatial multiplexing, and the low bit error rate increases the system's throughput [3-4]; Mutual coupling occurs when multiple antennas are put in close proximity in a MIMO system. The literature describes numerous techniques to enhance the isolation in MIMO antennas. These approaches are broadly categorized as suppressing coupling current and alternate current channels. Isolation enhancement techniques such as defected ground structure (DGS), meta-material loading, and filters behave as band-stop filters and suppress the coupling effect [5-14]. On the contrary, matching networks, neutralization line (NL), and embedding parasitic elements provide a local alternate current path,

so the coupling current should not reach the neighboring antenna element. An inset-fed rectangular two-port antenna operating in the UWB range is presented in [6]. An electromagnetic band gap arrangement between the antennas improves the isolation among the elements. In [8], an orthogonal configuration with the shared structure is proposed for the reduction of mutual coupling in the two-port MIMO antenna. The different structures and their impact on designing the UWB antenna are illustrated in [9]. In [10], a hybrid construction formed of a rectangle and a circular with a reduced ground plane illustrates UWB functionality. Furthermore, the designed antenna is placed orthogonally with the common ground plane to eliminate mutual interaction among the inter-components. Authors in [12] show microstrip fed rhombic shape slot antennas. The suggested design improves isolation by employing parasitic components and putting the antennas perpendicular to each other, allowing the coupling current to be neutralized. Two-port UWB MIMO antenna based on the NL is presented [14]. The suggested design cancels out the coupling current between the components by creating an out-of-phase current of equal magnitude. The literature reveals that most of the work employs decoupling structures such as defective ground structures, orthogonal antenna location, orientation, and loading parasitic components onto the radiator to improve isolation. Maintaining consistent radiation characteristics while designing a compact MIMO antenna with strong isolation and a broader impedance bandwidth is difficult.

This study provides a two-element MIMO design that operates in the UWB band. The physical dimension of the proposed design is 21.5×34×1.6 mm<sup>3</sup>, demonstrating an S11 ranging from 4.5 GHz to 13 GHz. The unique chain-structured parasitic element is

introduced between the components to function as a decoupling framework. The ground plane is adjusted to achieve the required reflection coefficient curve. The projected design has isolation better than the 18 dB across the bandwidth, diversity features are also examined, and results demonstrate their values are less than the minimum levels required for MIMO applications.

## II. MIMO ANTENNA DESIGN

### 1. Single Element Design

The conventional circular monopole antenna is designed with a radius of 5.6 mm, having a fullground plane to resonate at the frequency of 7.5 GHz. The designed antenna demonstrates the resonating frequency of 11 GHz due to poor impedance matching. To realize the UWB spectrum, the circular monopole antenna is modified by embedding an ellipse in between the feedline and radiator, and the ground plane is lowered. The reduction of a ground plane and modification to the circular radiator creates the current discontinuities and helps in realizing the UWB spectrum. The antenna design operates in the frequency range of 4-12 GHz with the realvalue of the impedance around 50Ω and an imaginary value of approximately zero as illustrated in Fig. 1.

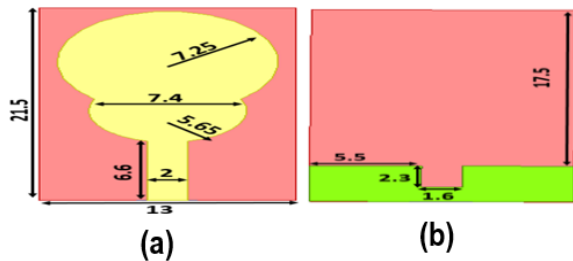


**Fig. 1.** The Projected circular monopole antenna (a) radiating (b) ground plane. (Dimensions are in mm).

The following equations are used to build a circular monopole antenna in the first step. The radius ( $r$ ) of the circular patch is determined by

$$r = \frac{F}{1 + \sqrt{\frac{2h}{\pi \epsilon r F [\ln(\frac{\pi F}{2h}) + 1.7726]}}} \quad (1)$$

Where  $F$  is given by,

$$F = \frac{8.791 \times 10^9}{f r \sqrt{\epsilon r}} \quad (2)$$

The fringing field spreads from the patch boundary to the ground plane, resulting in the effective radius. The fringing field around the circular patch may increase the radius of a circle. Therefore, the effective radius ( $r_{eff}$ ) is determined as shown below

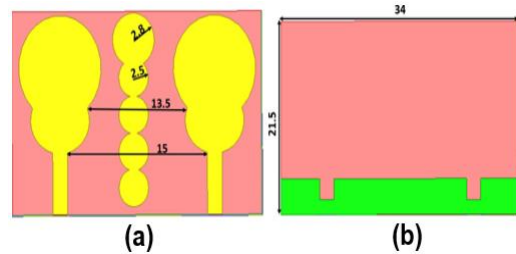
$$r_{eff} = \frac{1.8412c}{2\pi f r \sqrt{\epsilon r}} \quad (3)$$

Where  $C = 3 \times 10^{11}$  mm/sec.

### 2. Two Element MIMO Antenna Design

The UWB antenna is horizontally mirrored with a spacing of 10 mm (less than the quarter wavelength,  $\lambda$  calculated at the frequency of 4 GHz) to form a two-port UWB antenna. The ground plane of the single-element antenna is extended across the width of the substrate of the two-port antenna as illustrated in Fig. 2. This arrangement leads to poor isolation among the antenna elements. To enhance the isolation among the MIMO antenna elements, a unique chain-structured parasitic element called as neutralization line (NL) is installed as a

decoupling structure among the antennas of the MIMO system. The parasitic element creates local current channels that neutralize the coupling effect from the excited antenna and helps in isolation improvement as illustrated in Fig. 3. The two-port UWB antenna operates from 4.5 GHz to 13 GHz, providing an isolation of better than 20 dB across the impedance bandwidth except in the operating frequency range of 9-10 GHz, where isolation is better than 18 dB.



(a) radiating (b) ground plane. (Dimensions are in mm).

**Fig. 2.** The Projected two-port MIMO antenna

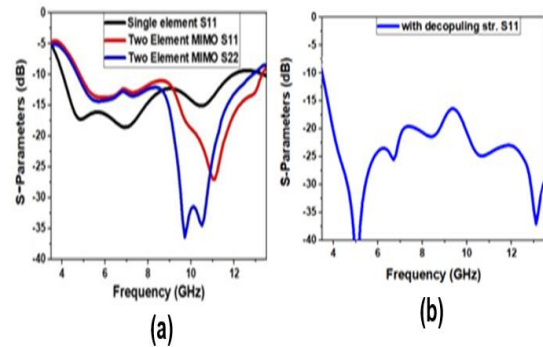


**Fig. 3.** The Projected two-port MIMO antenna (a) reflection coefficient (b) transmission coefficient.

The described design employs FR4 as a substrate. The physical size is  $0.4\lambda \times 0.5\lambda \times 0.02\lambda$ , resulting in impedance bandwidth ranging from 4.5-13 GHz. Following a thorough parametric analysis, the appropriate physical dimensions are determined.

### A. Surface Current Distribution

As demonstrated in Figure 4, the surface flow of current is presented at the resonant frequency of 9.7 GHz and 11 GHz. This is performed by activating one port and deactivating the other. The graphic demonstrates that the feedline, NL, and ground plane have the highest current concentration. The current concentration ensures that the NL prevents the coupling field from reaching the adjoining antenna, resulting in enhanced isolation.

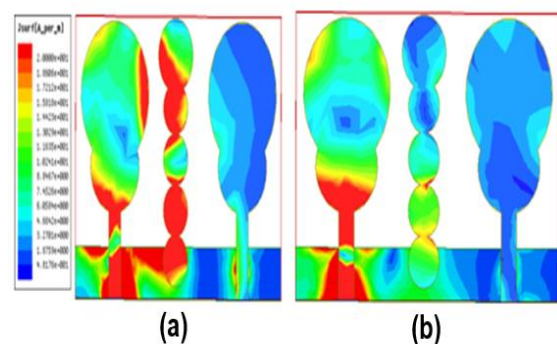


**Fig. 4.** The plots of surface current of the antenna (a) 9.7 GHz and (b) 11 GHz.

### 3. Parametric Investigation of Two-Port MIMO Antenna

#### A. Effect Decoupling Structure

The effect of decoupling structure is studied and is illustrated in Fig. 5. The results reveal that the minimum isolation  $S_{21}$  obtained without decoupling structure is 15 dB which is very low for a good MIMO antenna. After embedding a unique chain-structured parasitic element called as neutralization line (NL) as a decoupling structure among the antennas in the radiating part of the MIMO antenna the isolation is enhanced upto 20 dB.

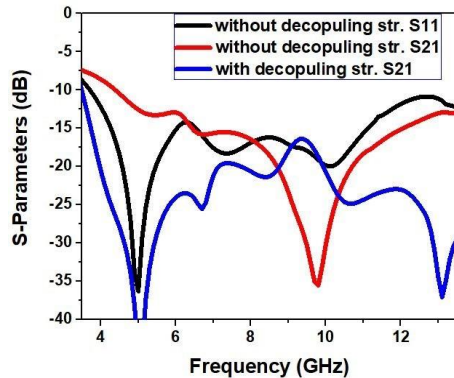


Fig. 5. Effect of decoupling structure.

#### B. Effect of distance between the elements

To fix the optimum distance between the element an analysis is performed on a connected ground plane MIMO structure where the distance between the two radiating elements is varied, and the effect of surface wave coupling is studied. Fig. 6 (a) indicates that at 9.5 mm, the minimum isolation obtained is 10 dB in the band of interest. For 11.5 mm, the isolation is best however the  $S_{11}$  and  $S_{22}$  are not optimum as can be seen in Fig. 6(b). At 13.5 mm, the structure resulted in better minimum isolation of 18 dB throughout the frequency of interest with co related  $S_{11}$  and  $S_{22}$  as illustrated in Fig. 6 (a) and (b), respectively.

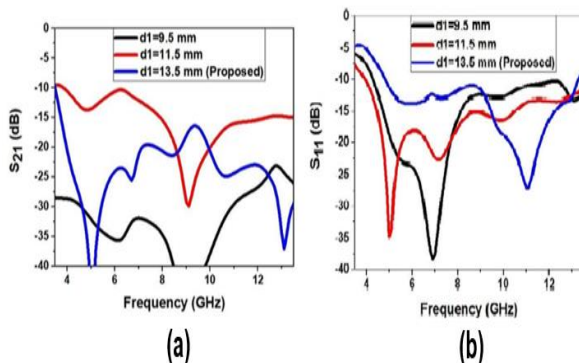


Fig. 6. Effect of distance between the elements (a) Isolation ( $S_{21}$ ) (b)  $S_{11}$  and  $S_{22}$ .

### III. RESULTS AND DISCUSSION

The proposed antenna is simulated in high-frequency structure simulation (HFSS) version 2014. The solution to the model is obtained using the finite element method (FEM) with a meshing of 0.333.

#### 1. Scattering parameters Gain and Radiation Pattern

The proposed antenna is fabricated and the prototype is illustrated in Fig. 7. The single-element antenna has generated impedance bandwidth ranging from 4-12 GHz. When the antenna is mirrored horizontally with connected ground to form a MIMO design it results in impedance

and width ranging from 4.5 -13 GHz under simulation and 4.7-12.8 GHz under measurement as illustrated in Figure 8. Also, it can be seen that the simulated and measured result are closely correlated with each other. The proposed antenna has good gain at the operating bands with 7.25 dB at 9.7 GHz and, 7.39 dB at 11 GHz, as illustrated in Figure 9. The two-port MIMO antenna radiation pattern is depicted in Figure 10, wherein it can be read that at both the operating frequency stable radiation performances are achieved.

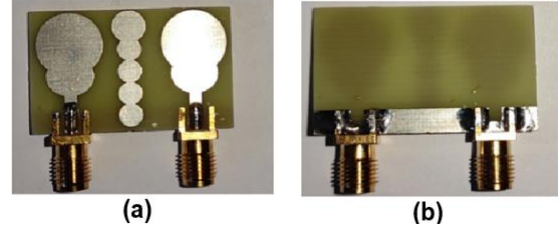


Fig. 7. The fabricated two-port MIMO antenna (a) radiating (b) ground plane.

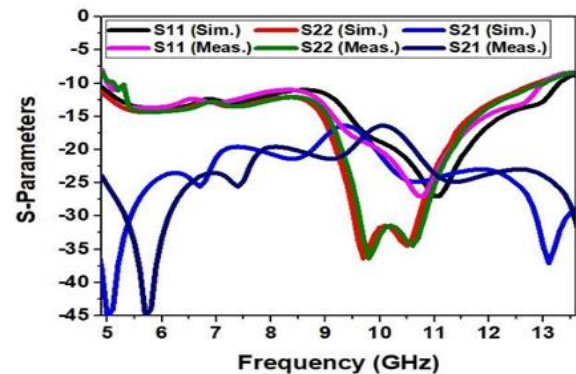


Fig. 8. Simulated and measured results  $S_{11}$  and isolation  $S_{21}$  of proposed MIMO antenna.

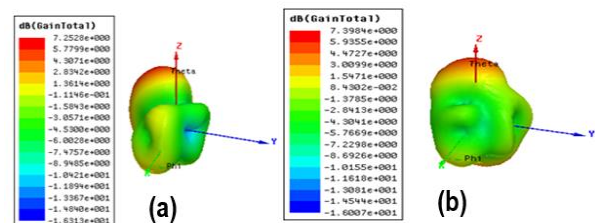


Fig. 9. 3D Gain of the two-port MIMO antenna at (a) 9.7 GHz and (b) 11 GHz.

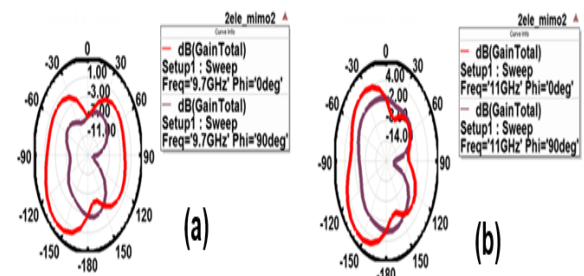


Fig. 10. Radiation pattern of proposed MIMO antenna at (a) 9.7 GHz and (b) 11 GHz.

#### 2. Diversity Parameters

MIMO antenna should satisfy certain diversity parameters such that the proposed design is accepted universally. We have calculated the ECC, DG, CCL, and TARC using the S- parameter approximation method.

Envelope Correlation Coefficient (ECC): ECC represents the radiation pattern independence from each MIMO element [19] and is mathematically calculated as given in equation 4. For the proposed MIMO antenna, obtained ECC is < 0.00142 for all the respective bands, as shown in Figure 11.

$$ECC = \frac{-\sum_{n=1}^N S_{ni}^* S_{nj}}{\sqrt{(1 - \sum_{n=1}^N |S_{ni}|^2)(1 - \sum_{n=1}^N |S_{nj}|^2)}} \quad (4)$$

Where  $S_{ni}$  and  $S_{nj}$  are s-parameters of the  $i^{th}$  and  $j^{th}$  ports.

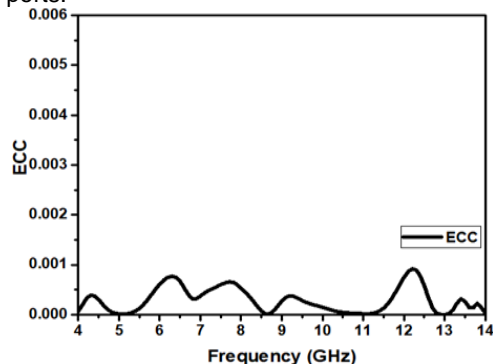


Fig. 11. ECC results of proposed MIMO antenna.

Directive Gain (DG): The MIMO antenna should have a comparatively high signal-to-noise ratio to that of a single element and is mathematically calculated as given in equation 5. The DG should be close to 10. For our design, the DG has resulted in 10 for all bands, as displayed in Fig. 12.

$$DG = 10\sqrt{1 - |ECC|^2} \quad (5)$$

Channel Capacity Loss (CCL): The MIMO antenna throughput is maximum when the bit error rate is low and is mathematically calculated as given in equation 6. For good design, the CLL should be less than 0.4b/s/Hz. The proposed MIMO antenna has a maximum CCL of 0.31b/s/Hz, as shown in Fig. 13.

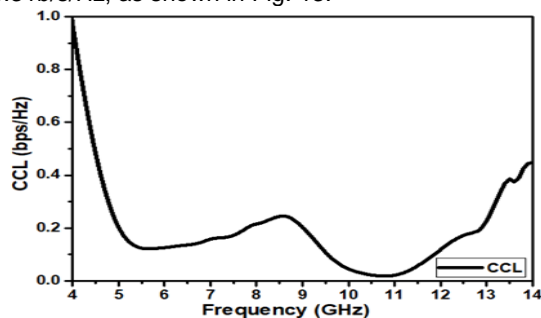


Fig. 12. CCL results of proposed MIMO antenna.

$$CCL = -\log_2(\alpha) \quad (6)$$

$$\alpha_{ii} = 1 - \left| \sum_{n=1}^N S_{in}^* S_{ni} \right| \text{ for } i, j = 1, 2, 3, 4,$$

$$\alpha_{ij} = 1 - \left| \sum_{n=1}^N S_{in}^* S_{nj} \right| \text{ for } i, j = 1, 2, 3, 4 \dots$$

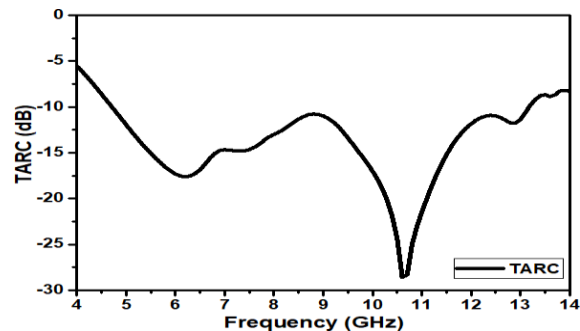


Fig. 13. TARC results of proposed MIMO antenna.

Mean effective gain (MEG): It depicts the antenna's average power ratio emitted to an incident concerning the isotropic environment and is mathematically calculated as given in equation 8 and is illustrated in Figure 14.

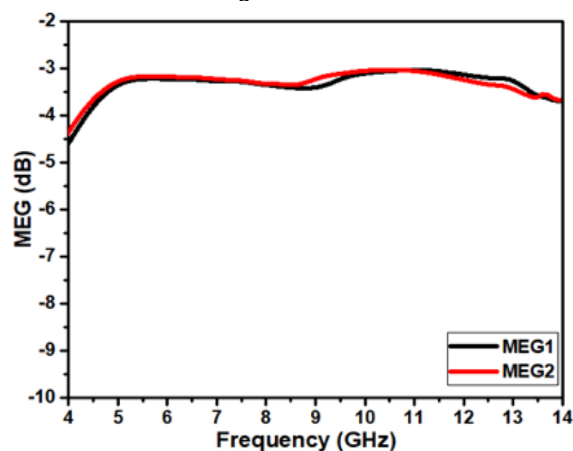


Fig. 14. MEG results of proposed MIMO antenna.

#### IV. CONCLUSION

This paper describes a two-port MIMO antenna with a neutralization line as a decoupling structure that operates in the UWB band. The unique chain-structured parasitic element form decoupling structure that links both antenna elements improves isolation between the antenna elements. The decoupling structure in the projected design creates an identical current having out of phase compared to the exciting antenna. Therefore it cancels the mutual coupling between antennas. The projected antenna shows stable radiation properties. Furthermore, the MIMO diversity parameters results verify that the MIMO antenna is suitable for the wireless communication system.

**Conflict of Interest.** The authors hereby confirm that there are no conflicts of interest.

#### REFERENCES

- [1]. Federal Communications Commission (FCC), (2002). Revision of part 15 of the commission's rules regarding ultra-wideband transmission systems," First Report and Order, ET Docket 98-153, FCC 02-48; Adopted: February 2002; Released: April 2002.
- [2]. P. Kumar, T. Ali, P. M. MM, (2021). Highly isolated ultrawideband multiple input and multiple output antenna for wireless applications, *Eng. sci.*, 17, pp. 83-90.

- [3]. S. Zhang and G. F. Pedersen (2016). Mutual coupling reduction for UWB MIMO antennas with a wideband neutralization line. *IEEE Antennas Wirel. Propag. Lett.*, 15, pp. 166–169.
- [4]. P. Kumar, M. M. M. Pai, and T. Ali, (2020). Metamaterials: New aspects in antenna design. *Telecommun. Radio Eng.*, vol. 79, no. 16, pp. 1467–1478.
- [5]. P. Kumar, M. M. M. Pai, and T. Ali, (2020). Ultrawideband antenna in wireless communication: A review and current state of the art. *Telecommun. Radio Eng.*, vol. 79, no. 11, pp. 929–942.
- [6]. A. Khan, S. Bashir, S. Ghafoor, and K. K. Qureshi, (2021). Mutual coupling reduction using ground stub and EBG in a compact wideband MIMO-antenna. *IEEE Access*, vol. 9, pp. 40972–40979.
- [7]. P. Kumar, T. Ali, and M. M. M. Pai, (2021). Electromagnetic metamaterials: A new paradigm of antenna design," *IEEE Access*, 9, pp. 18722–18751.
- [8]. L. Y. Nie, X. Q. Lin, S. Xiang, B. Wang, L. Xiao, and J. Y. Ye, (2020). High-isolation two-port UWB antenna based on shared structure. *IEEE Trans. Antennas Propag.*, vol. 68, no. 12, pp. 8186–8191.
- [9]. P. Kumar, M. M. M. Pai, and T. Ali, (2021). Design and analysis of multiple antenna structures for ultrawide bandwidth. *Telecommun. Radio Eng.*, 80, no. 6, pp. 41–53.
- [10]. A. A. Khan, S. A. Naqvi, M. S. Khan, and B. Ijaz, (2021). Quad port miniaturized MIMO antenna for UWB 11 GHz and 13 GHz frequency bands. *Int. J. Electron. Commun.*, 131, no. 153618, p. 153618.
- [11]. W. A. E. Ali and A. A. Ibrahim (2017). A compact double-sided MIMO antenna with an improved isolation for UWB applications," *Int. J. Electron. Commun.*, 82, pp. 7–13.
- [12]. Z. Chen, W. Zhou, and J. Hong (2021). A miniaturized MIMO antenna with triple band-notched characteristics for UWB applications. *IEEE Access*, 9, pp. 63646–63655.
- [13]. P. Kumar, T. Ali, and M. M. M. Pai (2020). A compact highly isolated two- and four-port ultrawideband Multiple Input and Multiple Output antenna with Wireless LAN and X-band notch characteristics based on Defected Ground Structure, *Int. J. Commun. Syst.*, 2022.
- [14]. P. Kumar, T. Ali, and M. M. M. Pai (2022). Characteristic Mode Analysis-Based Compact Dual Band-Notched UWB MIMO Antenna Loaded with Neutralization Line. *Micromachines*, 13, no. 10, p.1599.
- [15]. O. A. Shelar, T. Ali and P. Kumar (2022). UWB-MIMO antenna for wireless communication systems with isolation enhancement using metamaterial," 2022 16th European Conference on Antennas and Propagation (EuCAP), 2022, pp. 1-5, doi: 10.23919/EuCAP53622.2022.9769187.
- [16]. X. Tang, Z. Yao, Y. Li, W. Zong, G. Liu, and F. Shan (2021). A high performance UWB MIMO antenna with defected ground structure and U-shape branches," *Int. J. RF Microw. Comput-Aid. Eng.*, 31, no. 2.
- [17]. A. Bhattacharya, B. Roy, S. K. Chowdhury, and A. K. Bhattacharjee (2022). An isolation enhanced, printed, low-profile UWB-MIMO antenna with unique dual band-notching features for WLAN and WiMAX. *IETE J. Res.*, vol. 68, no. 1, pp. 496–503.
- [18]. S. Zhang and G. F. Pedersen (2016). Mutual coupling reduction for UWB MIMO antennas with a wideband neutralization line. *IEEE Antennas Wirel. Propag. Lett.*, 15, pp. 166–169.

**How to cite this article:** Satish Kumar Kannale and N. M. Biradar (2023). A novel Two-Port MIMO Antenna with Enhanced Isolation and Diversity Parameters for Wireless Applications. *International Journal on Emerging Technologies*, 14(1): 66–70.